


SHORT COMMUNICATION

## Exosome secretion promotes chemotaxis of cancer cells

Bong Hwan Sung <sup>a</sup> and Alissa M. Weaver<sup>a,b,c</sup>

<sup>a</sup>Department of Cancer Biology, School of Medicine, Vanderbilt University, Nashville, TN, USA; <sup>b</sup>Department of Cell and Developmental Biology, School of Medicine, Vanderbilt University, Nashville, TN, USA; <sup>c</sup>Department of Pathology, Microbiology, and Immunology, School of Medicine, Vanderbilt University, Nashville, TN, USA

### ABSTRACT

Migration of cells toward chemical cues, or chemotaxis, is important for many biologic processes such as immune defense, wound healing and cancer metastasis. Although chemotaxis is thought to occur in cancer cells, it is less well characterized than chemotaxis of professional immune cells such as neutrophils. Here, we show that cancer cell chemotaxis relies on secretion of exosome-type extracellular vesicles. Migration of fibrosarcoma cells toward a gradient of exosome-depleted serum was diminished by knockdown of the exosome secretion regulator Rab27a. Rescue experiments in which chemotaxis chambers were coated with purified extracellular vesicles demonstrate that exosomes but not microvesicles affect both speed and directionality of migrating cells. Chamber coating with purified fibronectin and fibronectin-depleted exosomes demonstrates that the exosome cargo fibronectin promotes cell speed but cannot account for the role of exosomes in promoting directionality of fibrosarcoma cell movement during chemotaxis. These experiments indicate that exosomes contain multiple motility-promoting cargoes that contribute to different aspects of cell motility.

### ARTICLE HISTORY

Received 15 August 2016  
Revised 26 October 2016  
Accepted 9 December 2016

### KEYWORDS

cell migration; chemotaxis; exosomes; extracellular vesicles; fibronectin

### Introduction

Exosomes are small extracellular vesicles that are secreted from late endosomal multivesicular endosomes. Exosome secretion was originally reported to occur in specialized cell types such as dendritic cells and reticulocytes.<sup>1–3</sup> However, recent reports indicate that exosomes are secreted from virtually all cell types, including normal and cancer cells, and play an important role in autocrine and paracrine communication.<sup>4,5</sup> Exosomes deliver bioactive cargos, including proteins, RNAs and lipids.<sup>4</sup> In cancer, exosomes have been shown to influence many tumor properties, including growth, angiogenesis, invasion, and metastasis.<sup>6–11</sup> Additional extracellular vesicles (EVs), known as microvesicles (MVs), are shed from the surface of cells and also have been implicated in numerous biologic phenotypes, including embryonic stem cell communication, oncogenic transformation, and inflammation.<sup>12–15</sup>

A major function of exosomes appears to be promotion of cell motility.<sup>6,10,16–18</sup> Thus, exosomes have been shown to promote cell protrusion formation,<sup>16</sup> adhesion,<sup>6,19</sup> and cell polarity.<sup>20</sup> In neutrophils, autocrine generation of bioactive lipids on exosomes

enhances motility toward the chemoattractant *N*-formyl-Methionyl-Leucyl-Phenylalanine (fMLP).<sup>21</sup> In a previous report,<sup>6</sup> we showed that inhibition of exosome secretion by knockdown of Rab27a, Synaptotagmin7 or Hrs in cancer cells inhibits *in vivo* metastasis and motility of cancer cells in a chick embryo model system. In this model, exosome secretion controlled both cell speed and directionality; however the directional cues were unclear. Using *in vitro* random motility assays, we showed that extracellular matrix carried by exosomes enhances adhesion assembly and is critical for cell speed. Our *in vitro* motility experiments did not reveal a defect in directional persistence of exosome secretion-inhibited cells; however there was no directional cue in those assays.

Chemotaxis is one type of directional cell locomotion, in which cells migrate toward a chemical stimulus. Activation of receptors, such as G protein-coupled chemokine receptors, mediates directed cell migration toward chemotactic cues.<sup>22,23</sup> Chemotaxis of cancer cells is thought to promote cancer metastasis.<sup>24–28</sup> For example, melanoma cells are directed out from tumors toward a higher level of a chemoattractant, lysophosphatidic acid,

to intravasate into local blood vessels.<sup>26</sup> Another example is metastasis of breast cancer cells to the lung, driven by SDF-1 and its receptor CXCR4 chemokine receptor 4 (CXCR4).<sup>27-29</sup> Recently, exosome secretion was shown to enhance chemotaxis of neutrophils and macrophages.<sup>21,30,31</sup> However, the role of exosome secretion in cancer cell chemotaxis is unknown.

Here, we explore the role of exosomes in cancer cell chemotaxis. Using exosome-depleted serum as a chemoattractant, we find that HT1080 fibrosarcoma cells inhibited for exosome secretion have a defect in directional migration up a chemical gradient. Using a rescue approach, in which chemotaxis chambers are coated with purified exosomes, MVs, or fibronectin (FN), we find that FN carried by exosomes promotes cell speed but cannot account for the role of exosomes in promoting directional movement toward chemoattractant.

## Results and discussion

To test whether exosome secretion affects cancer cell response to a chemoattractant gradient, we seeded control and Rab27a-knockdown (KD1, KD2) HT1080 fibrosarcoma cells in commercial chemotaxis chambers (ibidi), which generate stable gradients through diffusion.<sup>32</sup> After 5 h of adhesion, cells were given a gradient of 20–0% exosome-depleted serum and allowed to migrate for 12 h. Analysis of the time-lapse movies demonstrated that control cells migrated directionally toward the gradient (Fig. 1A). In contrast, Rab27a-KD cells had defects in both overall speed (Fig. 1A and B, no coating condition) and in directional cell movement (Fig. 1A, C, and D, no coating). Note that due to the defect in cell speed, most Rab27a-KD cell tracks in the Wind-Rose representation are overlapping in the low power view (Fig. 1A). Zooms of the central portion of each Wind-

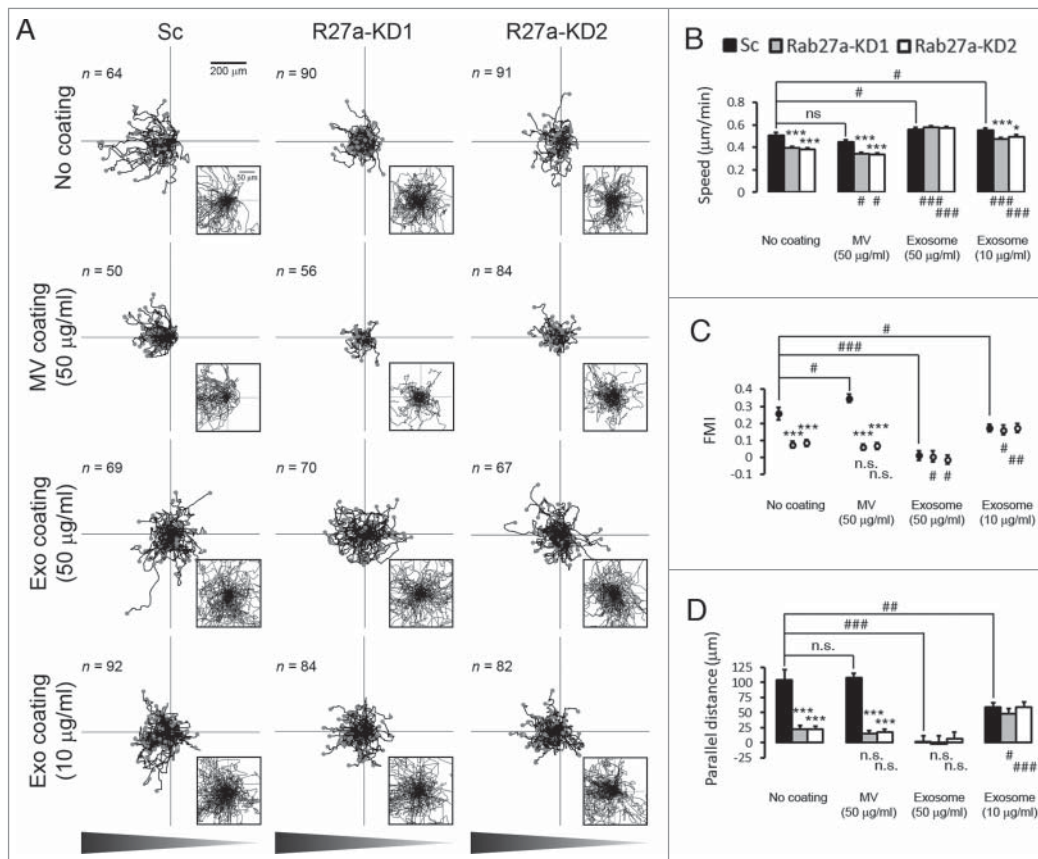


**Figure 1.** Exosome secretion promotes directional cell movement during chemotaxis. (A) Wind-Rose plots of cell tracks from scrambled shRNA control (Sc) and Rab27a-KD (R27a-KD) cells migrating in the chemotaxis chambers in the presence or absence of coated microvesicles (MV 50 µg/ml) or density gradient-purified exosomes (Exo 50 µg/ml and 10 µg/ml). Graphs are oriented such that the left side represents the direction of the chemoattractant gradient as shown in triangle bars below the panel. End points of migration tracks are marked with dots. Insets represent the enlarged zoom-in regions of the plots. (B–D) Quantification of cell migration characteristics from the cell tracks. (B) Cell speed. (C) Forward migration index (FMI). (D) Parallel distance. \* $p < 0.05$ ; \*\* $p < 0.01$ ; \*\*\* $p < 0.001$  compared with Sc under the same coating conditions. #  $p < 0.05$ ; ##  $p < 0.01$ ; ###  $p < 0.001$  compared with the same cell line on the No coating condition. n.s. = not significant. 2 to 3 regions were observed for each chamber and analyzed from 3 independent experiments. The number of cell tracks used for n value in statistics is shown in each panel in (A).

Rose plot show that most KD cell tracks are not directed in any direction while there is a skew in the control cell tracks toward the gradient (Fig. 1A, zooms). Forward migration index (FMI) and parallel distance specifically quantitate the movement of cells toward a chemoattractant (see Methods for details) and confirm the defect in Rab27a-KD cells in chemotaxis (Fig. 1C and D).

We previously found that coating tissue culture dishes with either fibronectin or purified exosomes could rescue the speed defects of Rab27a- or Hrs-KD cells in random motility.<sup>6</sup> We further found that fibronectin carried by exosomes promotes cell adhesion, explaining the speed defect of exosome secretion-inhibited cells.<sup>6</sup> To explore the role of EVs and their cargoes in cancer cell chemotaxis, we performed a similar approach. Exosomes were isolated from the conditioned media of HT1080 fibrosarcoma cells by serial centrifugation (ultracentrifuged exosomes, UC-Exo). We then further purified UC-Exo by sedimentation into a density gradient of Optiprep (DG-Exo) as described previously.<sup>6</sup> Consistent with our previous publication,<sup>6</sup> Western blot analysis revealed that FN is carried by HT1080 UC-Exo as well as DG-Exo but not on MV (Fig. 2A). FN was found in 3 density gradient fractions: Fractions 7, 9 and 10. Fraction 7 included the exosomal markers CD63 and TSG101, along with FN-binding receptor subunit, integrin  $\alpha 5$ . Conversely, Fractions 9 and 10 are more dense than fraction 7 and did not contain exosome markers suggesting that the FN in those fractions is in a fibrillar and/or aggregated form not associated with exosomes. Nanoparticle tracking analysis of DG-Exo Fraction 7 showed the expected size distribution for exosomes with a peak

diameter of 116 nm (Fig. 2B). Fraction 7 was used for all exosome-related assays. Likewise, MVs showed the expected larger size distribution, with multiple peak diameters of 158 nm, 218 nm and 395 nm.

To measure what proportion of the vesicle preparations is adherent under our experimental conditions, we counted MV and exosome number before and after coating 96 well plates using nanoparticle tracking analysis. The data indicate that approximately 80% of vesicles adhere to tissue culture-treated surfaces for both MV and exosomes (Fig. 2C). Pre-coating of the chemotaxis chamber migration surface with 50  $\mu\text{g/ml}$  MV did not affect any aspect of migration except for FMI of control cells, which was slightly increased (Fig. 1A–D). By contrast, coating the chemotaxis chambers with 50  $\mu\text{g/ml}$  exosomes fully rescued the speed defects of Rab27a-KD cells as well as slightly increasing the speed of control cells (Fig. 1B, Exosome 50  $\mu\text{g/ml}$ ). Interestingly, the exosome coating not only did not rescue directional movement defects of Rab27a-KD cells but also abolished chemotaxis of control cells (Fig. 1A, Exo coating 50  $\mu\text{g/ml}$ ). Thus, in this condition both control and Rab27-KD cells had FMI and parallel distance measurements near zero, indicating no bias toward the chemoattractant (Fig. 1C and D, Exosome 50  $\mu\text{g/ml}$ ). Since the exosomes were coated uniformly across the chamber, these data suggest that exosomes carry a component that enhances directional movement and can redirect cells in a chemical gradient when presented in a non-polarized manner.

To determine whether the high concentration of exosomes were saturating the surface and affecting the

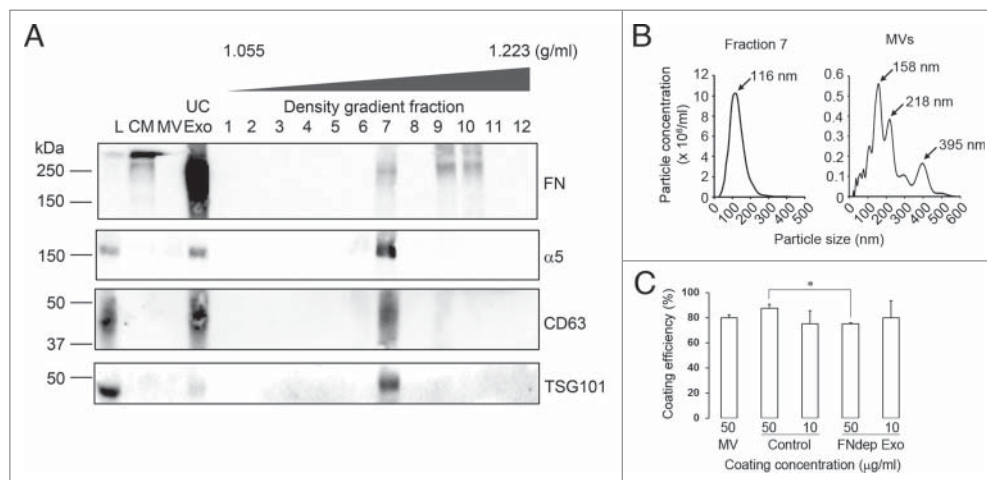


**Figure 2.** Characterization of extracellular vesicle preparations. Exosomes and MV were isolated from conditioned media (CM) using ultracentrifugation (UC-Exo). Exosomes were further purified using density gradient centrifugation. (A) Western blot analysis of the fractions (Density gradient fractions 1–12) for exosome markers CD63 and TSG101 identified Fraction 7 as the major peak containing exosomes. Both FN and its receptor  $\alpha 5$  integrin were present in the Fraction 7 exosome peak. FN was also present separate from exosome markers in Fractions 9 and 10. L = Total Cell Lysate, MV = Microvesicles. (B) NanoSight analysis of Fraction 7 showed a typical exosome size profile. The MV preparation also showed a typical size profile. (C) Exosome coating efficiency. MV = Microvesicles, Control = Regular exosomes, FNdep Exo = FN-depleted exosomes. \* $p < 0.05$ .

cellular response, we also tested a lower concentration of exosomes (10  $\mu\text{g/ml}$ ). This concentration slightly increased the speed of control cells and mostly rescued the speed defects of Rab27a-KD cells (Fig. 1B, Exosome 10  $\mu\text{g/ml}$ ). Similar to the 50  $\mu\text{g/ml}$  exosome coating, 10  $\mu\text{g/ml}$  exosome coating decreased both FMI and parallel distance of control cells compared with no coating, although to a lesser extent. However, the 10  $\mu\text{g/ml}$  exosome coating also slightly enhanced the ability of Rab27a-KD cells to undergo chemotaxis, increasing the FMI and parallel distance measurements up to those of control values (Fig. 1A, C, and D, Exosome 10  $\mu\text{g/ml}$ ). Thus for both coating concentrations, exosomes increase the cell speed of KD cells and equalize the response of control and KD cells to chemoattractant; however, the 10  $\mu\text{g/ml}$  concentration reduces the chemotaxis of control cells while increasing the chemotaxis of KD cells compared with the no coating condition. The respective decrease and increase of Rab27a-KD1 and -KD2 cell FMI on 50  $\mu\text{g/ml}$  and 10  $\mu\text{g/ml}$  exosome coatings compared with KD cell FMI on the no coating control was statistically significant (Fig. 1C and D, indicated by # symbols underneath the plots). These data suggest that exosomes carry a cargo that promotes cell directionality when secreted but when presented in a uniform manner (e.g. coating) can abolish the ability of cells to move directionally.

We previously showed that FN is a critical exosome cargo that controls the speed of HT1080 cells and is specifically targeted to exosomes by binding to integrins.<sup>6</sup> To confirm that FN is located on the exosome surface as would be expected, we used a dot blot assay that can distinguish EV surface proteins from lumen proteins based on permeabilization of EVs in 0.1% Tween-20.<sup>33,34</sup> The tetraspanin CD63 was used as a positive control, as it is a well-characterized exosomal surface protein. Using an antibody to the large extracellular loop, CD63 was detected in both detergent-free and -containing conditions (Fig. 3A). Similarly, FN was detected in detergent-free as well as detergent-containing conditions indicating that FN is bound on the exosome surface (Fig. 3A). Likewise, the integrin  $\alpha 5$  cytoplasmic tail was detected in detergent-containing but not in detergent-free conditions, indicating that  $\alpha 5$  has the expected topology in exosomes with the cytoplasmic tail located in the exosomal lumen and the extracellular domain should be available to bind FN (Fig. 3A).

To test whether FN as an exosome cargo could affect directional migration, FN was depleted from exosomes by culturing cells in FN-depleted media for 10 d and collecting exosomes (Fig. 3B), as in our previous publication.<sup>6</sup> We then tested whether these exosomes could rescue speed and/or chemotaxis. Unlike on regular

exosome coating, the migration speed of control cells on FN-depleted exosome coating was slightly decreased for both the high and low concentrations (Fig. 3D, FNdepExo 50  $\mu\text{g/ml}$  and 10  $\mu\text{g/ml}$ ). Consistent with our finding that FN carried by exosomes promotes cell speed, there was no rescue of the migration speed defects of Rab27a-KD cells. Similar to the control exosome coating condition (Fig. 1), FN-depleted exosome coating diminished directional migration of control cells toward the chemoattractant, although at the 50  $\mu\text{g/ml}$  concentration this effect was not as robust as the inhibition by control exosomes. (Fig. 3E and F: FNdepExo 50  $\mu\text{g/ml}$  and 10  $\mu\text{g/ml}$ , compare with Exosome coating in Fig. 1C and D). In the presence of FN-depleted exosome coating, KD cell chemotaxis overall remained dampened and similar to control cell chemotaxis (Fig. 3E, F). These data suggest that the presence or absence of FN in exosomes primarily affects cell speed and not directionality.

To further test whether FN could affect directionality in a chemoattractant gradient, we performed chemotaxis assays in chambers coated uniformly with a high concentration of FN (100  $\mu\text{g/ml}$ ). As expected, this coating rescued the speed defects of Rab27a-KD cells; however, it did not rescue their chemotaxis defects (Fig. 3C–F, FN coating 100  $\mu\text{g/ml}$ ). In addition, control cells seeded in FN-coated chambers continued to recognize and migrate toward the chemotactic gradient (Fig. 3C, FN coating 100  $\mu\text{g/ml}$ ), suggesting that FN is unlikely to be the exosome component that abolishes chemotaxis (Fig. 1). Altogether, these data indicate that exosome secretion critically contributes to both speed and directionality of migration. Whereas FN is a critical cargo for adhesion formation<sup>6</sup> and overall cell speed, another component or multiple components must primarily mediate the directional response.

The number of studies on exosomes and MVs has rapidly increased over the past decade. However, although several reports have reported molecular mechanisms of biogenesis, cargo sorting, and secretion of exosomes,<sup>34–39</sup> the molecular mechanisms by which exosomes regulate cell behaviors are still largely unknown. Our previous study showed that exosome secretion promotes speed, directionality and persistence of cancer cell migration *in vivo*. However, *in vitro* experiments without directional cues were only useful for investigating the role of exosomes in promoting cell speed.<sup>6</sup> In this study, we found that Rab27a-KD cancer cells have a defect in chemotaxis toward a gradient of exosome-depleted serum. Furthermore, we found that a uniform coating of the chamber surface with exosomes, but not MVs or FN, counteracts control cell chemotaxis. These data suggest that local autocrine exosome secretion contributes to the chemotactic response and that

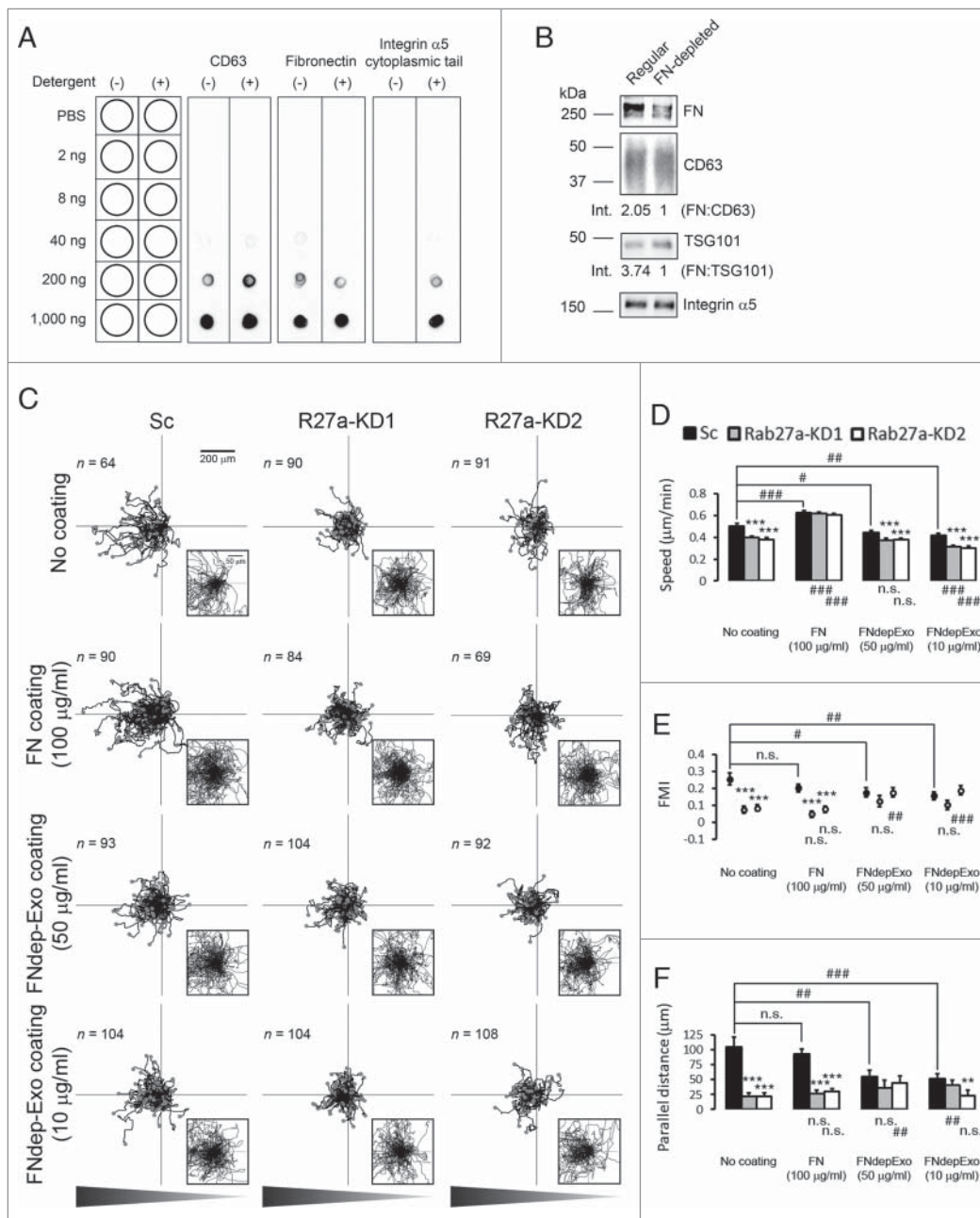


**Figure 3.** Fibronectin promotes speed but not directionality of cell migration during chemotaxis. (A) Dot blot analysis shows FN localized at the surface of exosomes. Notice that integrin  $\alpha 5$  was not detected by an antibody against its cytoplasmic tail in the absence of detergent. (B) Western blot analysis of FN depletion from exosomes. Equal numbers of control and FN-depleted exosomes were run side-by-side on the same gel. Note selective depletion of FN compared with exosomal markers, CD63 and TSG101 in FN-depleted exosomes. Numbers below the lanes indicate the ratio of FN to exosomal markers by densitometry analysis. (C) Wind-Rose plots of cell tracks from control (Sc) and Rab27a-KD (R27a-KD) cells migrating in the chemotaxis chambers in the presence or absence of coated FN (FN 100  $\mu\text{g/ml}$ ) or FN-depleted exosomes (FNdep-Exo 50  $\mu\text{g/ml}$  and 10  $\mu\text{g/ml}$ ). (D) Cell speed. (E) Forward migration index (FMI). (F) Parallel distance. \* $p < 0.05$ ; \*\* $p < 0.01$ ; \*\*\* $p < 0.001$  compared with Sc under the same coating conditions. #  $p < 0.05$ ; ##  $p < 0.01$ ; ###  $p < 0.001$  compared with the same cell line on the No coating condition. n.s. = not significant. 2 to 3 regions were observed for each chamber and analyzed from 3 independent experiments. The number of cell tracks used for  $n$  value in statistics is shown in each panel in (C).

exosomes contain directional cues. Cellular detection of any local exosome concentration differences is likely prevented by the presence of a high uniform concentration of exosomes.

Exosomes contain numerous cargoes including growth factors, chemokines, ECM proteins, receptors, and proteases, which could impact diverse aspects of cell motility.<sup>6,9,10,16,18</sup> We previously demonstrated that FN,

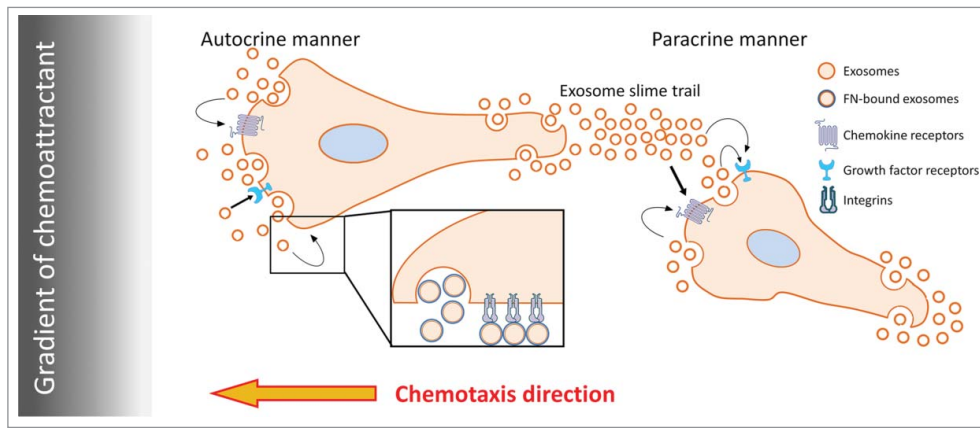


**Figure 4.** Proposed model for the role of exosome secretion in cancer cell chemotaxis. Soluble factors delivered in a gradient induce cell polarization and/or polarized secretion of exosomes. Exosomes secreted from cancer cells may deliver growth factors,<sup>18</sup> chemokines,<sup>21</sup> and ECM proteins including FN.<sup>6</sup> Exosome-carried cargoes, such as chemokines and/or growth factors, may provide positive feedback to promote directional sensing and migration toward chemoattractant in an autocrine manner. By contrast, exosomal ECM promotes cell speed. In a paracrine manner, exosome slime trails left behind migrating leader cells<sup>6,43</sup> could promote chemotaxis of follower cells.

as an exosome cargo, promotes HT1080 cell speed.<sup>6</sup> In this report, we confirmed that finding and further observed that FN does not appear to play a major role in controlling cell directionality. Instead it seems likely that other molecules, such as chemokines, lipid mediators, or other molecules, could be carried on cancer cell exosomes and drive cancer cell chemotaxis. Chemokine-containing exosomes derived from heat-stressed tumor cells are known to be chemoattractant to dendritic cells.<sup>40</sup> Majumdar et al.<sup>21</sup> reported that exosomes secreted from neutrophils synthesize and carry the chemoattractant leukotriene B<sub>4</sub> (LTB<sub>4</sub>). This LTB<sub>4</sub> on exosomes facilitates chemotaxis of neutrophils toward fMLP in both an autocrine and paracrine manner. Although we have not yet identified the exosome cargo that drives autocrine chemotaxis of HT1080 fibrosarcoma cells, our data are consistent with those previous findings and suggest that multiple exosome cargoes work together to facilitate different aspects of migration (See model in Fig. 4). Future studies should elucidate those cargoes. We also expect that in other cancer cell types, other ECM cargoes might have a similar effect as FN, promoting cell speed but not chemotaxis. This is an important hypothesis to test for the future. Altogether, we conclude that autocrine secretion of exosomes is an essential contributory process to cell motility, promoting cell adhesion and directionality.

## Methods

### Cell culture and reagents

HT1080 cells were maintained in DMEM supplemented with 10% bovine growth serum (BGS, SH30541.03,

HyClone). A lentiviral shRNA expression system, pLKO.1, was used to knockdown Rab27a (TRCN0000005296 and TRCN0000005297, Thermo Scientific) or scrambled control (Addgene).<sup>6</sup> FN was depleted from BGS using Gelatin Sepharose™ 4B (17-0956-01, GE Healthcare), as described previously.<sup>41</sup> To prepare exosome-depleted BGS for chemotaxis assays, BGS was ultracentrifuged at 100,000 x g overnight with a Ti45 fixed angle rotor (Beckman) and the supernatant was collected as exosome-depleted BGS. Anti-FN (610077, BD Biosciences, 1:1,000 dilution), anti-TSG101 (GTX70255, GeneTex, 1:500 dilution), anti-integrin  $\alpha$ 5 cytoplasmic tail (AB1928, Millipore, 1:5,000 dilution), and anti-CD63 (ab68418 for Western blotting, 1:500 dilution and ab8219 for Dot blotting, abcam, 1:500 dilution) were used. HRP-conjugated goat secondary antibodies (sc-2055 and sc-2054 for mouse and rabbit primary antibodies, respectively, 1:10,000 dilution) were from Santa Cruz Biotechnology. Blots were developed using a mix of Pierce™ ECL Western Blotting Substrate (32106, ThermoFisher Scientific) and SuperSignal™ West Femto Maximum Sensitivity Substrate (34905, ThermoFisher Scientific) and imaged using a ChemiDoc MP (Bio-Rad).

### Isolation of exosomes

To collect conditioned media, 80% confluent cells were cultured for 48 h in Opti-MEM. Exosomes were isolated from conditioned media by serial centrifugation at 300 x g for 10 min, 2000 x g for 30 min, 10,000 x g for 30min (9300 rpm in Ti45 rotor), and 100,000 x g (30,000 rpm in Ti45 rotor) for overnight to respectively sediment live cells, dead cells and debris, MVs, and exosomes. For further purification of ultracentrifuged exosomes, a discontinuous iodixanol gradient was prepared.<sup>42</sup> 40% (w/v),

20% (w/v), 10% (w/v), and 5% (w/v) solutions of iodixanol were made by diluting OptiPrep™ (60% (w/v) aqueous iodixanol, 1114542, Axis-Shield PoC) with 0.25 M sucrose/10 mM Tris, pH 7.5 from the bottom to the top of a 14 × 89 mm polyallomer tube. Ultracentrifuged-exosomes were added on a top of the gradient and continuous gradient was made through ultracentrifugation at 100,000 × g (24,000 rpm in SW40 Ti rotor) for 18 h. 12 fractions were collected and each fraction was diluted in PBS. Each fraction was pelleted through another round of ultracentrifugation at 100,000 × g for 3 h, washed with PBS, and resuspended in PBS. Exosome presence in fraction #7 was confirmed by Western blotting and used for experiments. All Western blotting samples were lysed in 5x SDS sample buffer (250 mM Tris-HCl, pH 6.8, 10% SDS, 50% glycerol, 0.05% bromophenol blue, 500 mM β-mercaptoethanol) Number and size distribution of exosomes was measured by nanoparticle tracking analysis with a NanoSight LM10 (Malvern). To deplete FN in exosomes, cells were cultured in DMEM supplemented with 10% FN-depleted BGS for 10 d before collecting conditioned medium for exosome isolation.<sup>6</sup> FN depletion from exosomes was confirmed by Western blotting using anti-FN antibody along with exosomal markers. Protein quantity was measured using Micro BCA Protein Assay Kit (23235, Thermo Scientific) after exosomes were lysed in 1% sodium dodecyl sulfate (final concentration).

### Chemotaxis assay

Cell migration toward a gradient of exosome-depleted BGS was performed in μ-Slide Chemotaxis<sup>3D</sup> chambers (80326, ibidi). For coating experiments, the cell observation area of the chamber was coated with microvesicles, exosomes, or human plasma fibronectin (33016–015, Life Technologies) suspensions in PBS at 4°C overnight before washing and using. Trypsinized cells were loaded into the cell observation area and cultured in DMEM supplemented with 10% exosome-depleted BGS for 5 to 6 hours to allow attachment. Then, cells were washed with serum-free Leibovitz's L-15 (21083–027, Gibco). A gradient of exosome-depleted BGS was made by diluting exosome-depleted BGS in Leibovitz's L-15 to a final concentration of 10% in the left reservoir of the chamber whereas serum-free Leibovitz's L-15 was present in the right reservoir. For coating experiments, 6 μl of each coating reagent (MVs, regular and FN-depleted exosomes, and fibronectin) was loaded to the observation area of the chemotaxis chamber and incubated at 4°C for overnight. Before cells were loaded, the chamber was equilibrated to room temperature and the observation area was washed with DMEM 3 times according to the manufacturer's

instructions. Time lapse images of migrating cells were captured at every 10 min for 12 h using a Nikon Eclipse TE2000E microscope equipped with a 37°C chamber. The nuclear position of each cell was tracked using ImageJ (Manual Tracking Plugins) and cell speed and forward migration index (FMI) were measured using the Chemotaxis and Migration Tool (ibidi). The formula of FMI is shown below modified from Instructions Chemotaxis and Migration Tool 2.0 (ibidi). Parallel distance was measured with distance of end points from start points of cell migration in the parallel direction.

$$FMI = \frac{1}{n} \sum_{i=1}^n \frac{\text{parallel distance}_i}{\text{accumulated distance}_i} \quad (1)$$

### Quantitation of exosome coating efficiency

To estimate the exosome coating efficiency, the exosome number/ml for 2 different concentrations of regular and FN-depleted exosomes (10 μg/ml and 50 μg/ml, diluted from all more concentrated stock) was quantitated by NanoSight LM10 before and after coating onto 96-well plates at 4°C for overnight. The percentage of exosome coating was calculated by

$$\frac{(n_{\text{before}} - n_{\text{after}})}{n_{\text{before}}} * 100 \quad (2)$$

where  $n_{\text{before}}$  is the exosome number in 7 μl solution before incubation and  $n_{\text{after}}$  is the exosome number in the collected solution after overnight incubation. The coating volume 7 μl was determined proportionally to the coating volume on the chemotaxis chamber (6 μl onto 0.27 cm<sup>2</sup> of coating area on the chemotaxis chamber vs. 7 μl onto 0.32 cm<sup>2</sup> of well area on the 96-well plate).

### Dot blot analysis

Various concentrations of isolated exosomes were absorbed onto nitrocellulose membranes at room temperature for 30 min. The membranes were blocked with 5% non-fat milk in PBS in the absence or presence 0.1% (v/v) Tween-20 (PBST) at room temperature for 1 h. Anti-fibronectin, anti-integrin α5 cytoplasmic tail, and anti-CD63 extracellular loop antibodies were incubated on the membranes in PBS or PBST blocking buffer at 4°C overnight followed by HRP-conjugated secondary antibody incubation at room temperature for 1 h. Blots were imaged using a ChemiDoc MP (Bio-Rad).

## Numbers and statistics

For quantitative data from experiments, the *n* values and independent experiment numbers are listed in the figure legends or on the figures. Data sets were compared using Student *t*-test in Microsoft Excel software and plotted as mean ± standard error in bar graphs or in scatter plots (FMI) using Microsoft Excel software.

## Disclosure of potential conflicts of interest

No potential conflicts of interest were disclosed.

## Funding

This work was funded by NIH grants 1R01CA206458, 1R01GM117916, and 1R01CA163592 to AMW.

## ORCID

Bong Hwan Sung  <http://orcid.org/0000-0002-8140-4685>

## References

- [1] Harding C, Heuser J, Stahl P. Receptor-mediated endocytosis of transferrin and recycling of the transferrin receptor in rat reticulocytes. *J Cell Biol* 1983; 97:329-39; PMID:6309857; <http://dx.doi.org/10.1083/jcb.97.2.329>
- [2] Pan BT, Johnstone RM. Fate of the transferrin receptor during maturation of sheep reticulocytes in vitro: selective externalization of the receptor. *Cell* 1983; 33:967-78; PMID:6307529; [http://dx.doi.org/10.1016/0092-8674\(83\)90040-5](http://dx.doi.org/10.1016/0092-8674(83)90040-5)
- [3] Zitvogel L, Regnault A, Lozier A, Wolfers J, Flament C, Tenza D, Ricciardi-Castagnoli P, Raposo G, Amigorena S. Eradication of established murine tumors using a novel cell-free vaccine: dendritic cell-derived exosomes. *Nat Med* 1998; 4:594-600; PMID:9585234; <http://dx.doi.org/10.1038/nm0598-594>
- [4] Colombo M, Raposo G, Thery C. Biogenesis, secretion, and intercellular interactions of exosomes and other extracellular vesicles. *Annu Rev Cell Dev Biol* 2014; 30:255-89; PMID:25288114; <http://dx.doi.org/10.1146/annurev-cellbio-101512-122326>
- [5] Zhang HG, Grizzle WE. Exosomes: a novel pathway of local and distant intercellular communication that facilitates the growth and metastasis of neoplastic lesions. *Am Pathol* 2014; 184:28-41; PMID:24269592
- [6] Sung BH, Ketova T, Hoshino D, Zijlstra A, Weaver AM. Directional cell movement through tissues is controlled by exosome secretion. *Nat Commun* 2015; 6:7164; PMID:25968605
- [7] Hoshino A, Costa-Silva B, Shen TL, Rodrigues G, Hashimoto A, Tesic Mark M, Molina H, Kohsaka S, Di Giannatale A, Ceder S, et al. Tumour exosome integrins determine organotropic metastasis. *Nature* 2015; 527:329-35; PMID:26524530; <http://dx.doi.org/10.1038/nature15756>
- [8] Peinado H, Aleckovic M, Lavotshkin S, Matei I, Costa-Silva B, Moreno-Bueno G, Hergueta-Redondo M, Williams C, Garcia-Santos G, Ghajar C, et al. Melanoma exosomes educate bone marrow progenitor cells toward a pro-metastatic phenotype through MET. *Nat Med* 2012; 18:883-91; PMID:22635005; <http://dx.doi.org/10.1038/nm.2753>
- [9] Hoshino D, Kirkbride KC, Costello K, Clark ES, Sinha S, Grega-Larson N, Tyska MJ, Weaver AM. Exosome secretion is enhanced by invadopodia and drives invasive behavior. *Cell Rep* 2013; 5:1159-68; PMID:24290760; <http://dx.doi.org/10.1016/j.celrep.2013.10.050>
- [10] Mu W, Rana S, Zoller M. Host matrix modulation by tumor exosomes promotes motility and invasiveness. *Neoplasia* 2013; 15:875-87; PMID:23908589; <http://dx.doi.org/10.1593/neo.13786>
- [11] Costa-Silva B, Aiello NM, Ocean AJ, Singh S, Zhang H, Thakur BK, Becker A, Hoshino A, Mark MT, Molina H, et al. Pancreatic cancer exosomes initiate pre-metastatic niche formation in the liver. *Nat Cell Biol* 2015; 17:816-26; PMID:25985394; <http://dx.doi.org/10.1038/ncb3169>
- [12] Desrochers LM, Bordeleau F, Reinhart-King CA, Cerione RA, Antonyak MA. Microvesicles provide a mechanism for intercellular communication by embryonic stem cells during embryo implantation. *Nat Commun* 2016; 7:11958; PMID:27302045; <http://dx.doi.org/10.1038/ncomms11958>
- [13] Zhang HM, Li Q, Zhu X, Liu W, Hu H, Liu T, Cheng F, You Y, Zhong Z, Zou P, et al. miR-146b-5p within BCR-ABL1-positive microvesicles promotes leukemic transformation of hematopoietic cells. *Cancer Res* 2016; 76:2901-11; PMID:27013199
- [14] Cumpelik A, Ankli B, Zecher D, Schifferli JA. Neutrophil microvesicles resolve gout by inhibiting C5a-mediated priming of the inflammasome. *Ann Rheum Dis* 2016; 75:1236-45; PMID:26245757; <http://dx.doi.org/10.1136/annrheumdis-2015-207338>
- [15] Raposo G, Stoorvogel W. Extracellular vesicles: exosomes, microvesicles, and friends. *J Cell Biol* 2013; 200:373-83; PMID:23420871; <http://dx.doi.org/10.1083/jcb.201211138>
- [16] Luga V, Zhang L, Vitoria-Petit AM, Ogunjimi AA, Inanlou MR, Chiu E, Buchanan M, Hosein AN, Basik M, Wrana JL. Exosomes mediate stromal mobilization of autocrine Wnt-PCP signaling in breast cancer cell migration. *Cell* 2012; 151:1542-56; PMID:23260141; <http://dx.doi.org/10.1016/j.cell.2012.11.024>
- [17] Ma L, Li Y, Peng J, Wu D, Zhao X, Cui Y, Chen L, Yan X, Du Y, Yu L. Discovery of the migrasome, an organelle mediating release of cytoplasmic contents during cell migration. *Cell research* 2015; 25:24-38; PMID:25342562
- [18] Higginbotham JN, Demory Beckler M, Gephart JD, Franklin JL, Bogatcheva G, Kremers GJ, Piston DW, Ayers GD, McConnell RE, Tyska MJ, et al. Amphiregulin exosomes increase cancer cell invasion. *Curr Biol* 2011; 21:779-86; PMID:21514161; <http://dx.doi.org/10.1016/j.cub.2011.03.043>
- [19] Fedele C, Singh A, Zerlanko BJ, Iozzo RV, Languino LR. The alphavbeta6 integrin is transferred intercellularly via exosomes. *J Biol Chem* 2015; 290:4545-51; PMID:25568317; <http://dx.doi.org/10.1074/jbc.C114.617662>



- [20] Lakkaraju A, Rodriguez-Boulant E. Itinerant exosomes: emerging roles in cell and tissue polarity. *Trend Cell Biol* 2008; 18:199-209; PMID:18396047; <http://dx.doi.org/10.1016/j.tcb.2008.03.002>
- [21] Majumdar R, Tavakoli Tameh A, Parent CA. Exosomes Mediate LTB4 Release during Neutrophil Chemotaxis. *PLoS Biol* 2016; 14:e1002336; PMID:26741884; <http://dx.doi.org/10.1371/journal.pbio.1002336>
- [22] Murphy PM. Chemokines and the molecular basis of cancer metastasis. *Eng J Med* 2001; 345:833-5; PMID:11556308
- [23] Janetopoulos C, Firtel RA. Directional sensing during chemotaxis. *FEBS Lett* 2008; 582:2075-85; PMID:18452713; <http://dx.doi.org/10.1016/j.febslet.2008.04.035>
- [24] Shields JD, Fleury ME, Yong C, Tomei AA, Randolph GJ, Swartz MA. Autologous chemotaxis as a mechanism of tumor cell homing to lymphatics via interstitial flow and autocrine CCR7 signaling. *Cancer Cell* 2007; 11:526-38; PMID:17560334; <http://dx.doi.org/10.1016/j.ccr.2007.04.020>
- [25] O'Boyle G, Swidenbank I, Marshall H, Barker CE, Armstrong J, White SA, Fricker SP, Plummer R, Wright M, Lovat PE. Inhibition of CXCR4-CXCL12 chemotaxis in melanoma by AMD11070. *Br J Cancer* 2013; 108:1634-40; PMID:23538388; <http://dx.doi.org/10.1038/bjc.2013.124>
- [26] Muinonen-Martin AJ, Susanto O, Zhang Q, Smethurst E, Faller WJ, Veltman DM, Kalna G, Lindsay C, Bennett DC, Sansom OJ, et al. Melanoma cells break down LPA to establish local gradients that drive chemotactic dispersal. *PLoS Biol* 2014; 12:e1001966; PMID:25313567; <http://dx.doi.org/10.1371/journal.pbio.1001966>
- [27] Sobolik T, Su YJ, Wells S, Ayers GD, Cook RS, Richmond A. CXCR4 drives the metastatic phenotype in breast cancer through induction of CXCR2 and activation of MEK and PI3K pathways. *Mol Biol Cell* 2014; 25:566-82; PMID:24403602; <http://dx.doi.org/10.1091/mbc.E13-07-0360>
- [28] Muller A, Homey B, Soto H, Ge N, Catron D, Buchanan ME, McClanahan T, Murphy E, Yuan W, Wagner SN, et al. Involvement of chemokine receptors in breast cancer metastasis. *Nature* 2001; 410:50-6; PMID:11242036; <http://dx.doi.org/10.1038/35065016>
- [29] Douglass S, Meeson AP, Overbeck-Zubrzycka D, Brain JG, Bennett MR, Lamb CA, Lennard TW, Browell D, Ali S, Kirby JA. Breast cancer metastasis: demonstration that FOXP3 regulates CXCR4 expression and the response to CXCL12. *J Pathol* 2014; 234:74-85; PMID:24870556; <http://dx.doi.org/10.1002/path.4381>
- [30] Esser J, Gehrman U, D'Alexandri FL, Hidalgo-Estevez AM, Wheelock CE, Scheynius A, Gabrielsson S, Radmark O. Exosomes from human macrophages and dendritic cells contain enzymes for leukotriene biosynthesis and promote granulocyte migration. *J Allerg Clin Immunol* 2010; 126:1032-40, 40 e1-4.
- [31] Kulshreshtha A, Ahmad T, Agrawal A, Ghosh B. Proinflammatory role of epithelial cell-derived exosomes in allergic airway inflammation. *J Allerg Clin Immunol* 2013; 131:1194-203, 203 e1-14.
- [32] Zengel P, Nguyen-Hoang A, Schildhammer C, Zantl R, Kahl V, Horn E.  $\mu$ -Slide Chemotaxis: a new chamber for long-term chemotaxis studies. *BMC Cell Biol* 2011; 12:21; PMID:21592329; <http://dx.doi.org/10.1186/1471-2121-12-21>
- [33] Lai CP, Kim EY, Badr CE, Weissleder R, Mempel TR, Tannous BA, Breakefield XO. Visualization and tracking of tumour extracellular vesicle delivery and RNA translation using multiplexed reporters. *Nat Commun* 2015; 6:7029; PMID:25967391
- [34] McKenzie AJ, Hoshino D, Hong NH, Cha DJ, Franklin JL, Coffey RJ, Patton JG, Weaver AM. KRAS-MEK signaling controls Ago2 sorting into exosomes. *Cell Rep* 2016; 15:978-87; PMID:27117408; <http://dx.doi.org/10.1016/j.celrep.2016.03.085>
- [35] Baietti MF, Zhang Z, Mortier E, Melchior A, Degeest G, Geeraerts A, Ivarsson Y, Depoortere F, Coomans C, Vermeiren E, et al. Syndecan-syntenin-ALIX regulates the biogenesis of exosomes. *Nat Cell Biol* 2012; 14:677-85; PMID:22660413; <http://dx.doi.org/10.1038/ncb2502>
- [36] Edgar JR, Eden ER, Futter CE. Hrs- and CD63-dependent competing mechanisms make different sized endosomal intraluminal vesicles. *Traffic* 2014; 15:197-211; PMID:24279430; <http://dx.doi.org/10.1111/tra.12139>
- [37] Hyenne V, Apaydin A, Rodriguez D, Spiegelhalter C, Hoff-Yoessle S, Diem M, Tak S, Lefebvre O, Schwab Y, Goetz JG, et al. RAL-1 controls multivesicular body biogenesis and exosome secretion. *J Cell Biol* 2015; 211:27-37; PMID:26459596; <http://dx.doi.org/10.1083/jcb.201504136>
- [38] Ostrowski M, Carmo NB, Krumeich S, Fanget I, Raposo G, Savina A, Moita CF, Schauer K, Hume AN, Freitas RP, et al. Rab27a and Rab27b control different steps of the exosome secretion pathway. *Nat Cell Biol* 2010; 12:19-30; sup pp 1-13; PMID:19966785; <http://dx.doi.org/10.1038/ncb2000>
- [39] Sinha S, Hoshino D, Hong NH, Kirkbride KC, Grega-Larson NE, Seiki M, Tyska MJ, Weaver AM. Cortactin promotes exosome secretion by controlling branched actin dynamics. *J Cell Biol* 2016; 214:197-213; PMID:27402952; <http://dx.doi.org/10.1083/jcb.201601025>
- [40] Chen T, Guo J, Yang M, Zhu X, Cao X. Chemokine-containing exosomes are released from heat-stressed tumor cells via lipid raft-dependent pathway and act as efficient tumor vaccine. *J Immunol* 2011; 186:2219-28; PMID:21242526
- [41] Sung BH, Zhu X, Kaverina I, Weaver AM. Cortactin controls cell motility and lamellipodial dynamics by regulating ECM secretion. *Curr Biol* 2011; 21:1460-9; PMID:21856159; <http://dx.doi.org/10.1016/j.cub.2011.06.065>
- [42] Tauro BJ, Greening DW, Mathias RA, Ji H, Mathivanan S, Scott AM, Simpson RJ. Comparison of ultracentrifugation, density gradient separation, and immunoaffinity capture methods for isolating human colon cancer cell line LIM1863-derived exosomes. *Methods* 2012; 56:293-304; PMID:22285593; <http://dx.doi.org/10.1016/j.ymeth.2012.01.002>
- [43] Kriebel PW, Barr VA, Rericha EC, Zhang G, Parent CA. Collective cell migration requires vesicular trafficking for chemoattractant delivery at the trailing edge. *J Cell Biol* 2008; 183:949-61; PMID:19047467; <http://dx.doi.org/10.1083/jcb.200808105>